By choosing a Φ and incrementing δ from $-90°$ to $+90°$, a curve of constant Φ can be computed from Eq (30) It should be noted that, for every value of δ used in Eq (30), two values of $(\alpha_L - \alpha)$ will be obtained Both points lie on the same Φ curve, however, and so there is no problem in computing the curve

The curves of constant A_L are not obtained so directly From Eq (17),

$$\sin A_L = - \frac{\cos\delta_s \sin(\alpha_L - \alpha)}{(1 - \cos^2\Phi)^{1/2}} \tag{31}$$

since

$$\cos^2\Phi + \sin^2\Phi = 1 \tag{32}$$

or

$$(1 - \cos^2\Phi)^{1/2} = - \frac{\cos\delta_s \sin(\alpha_L - \alpha)}{\sin A_L} \tag{33}$$

Squaring,

$$1 - \cos^2\Phi = \frac{\cos^2\delta \sin^2(\alpha_L - \alpha_s)}{\sin^2 A_L} \tag{34}$$

From Eq (14),

$$1 - (\cos\delta_L \cos\delta \cos(\alpha_L - \alpha) + \sin\delta_L \sin\delta)^2 = \cos^2\delta \sin^2(\alpha_L - \alpha)/\sin^2 A_L \tag{35}$$

Expanding

$$1 - (\cos^2\delta_L \cos^2\delta \cos^2(\alpha_L - \alpha) + 2\cos\delta_L \cos\delta \cos(\alpha_L - \alpha) \sin\delta_L \sin\delta + \sin^2\delta_L \sin^2\delta) = \cos^2\delta \sin^2(\alpha_L - \alpha)/\sin^2 A_L \tag{36}$$

$$\sin^2 A_L - \sin^2 A_L \cos^2\delta_L \cos^2\delta \cos^2(\alpha_L - \alpha) - 2\sin^2 A_L \cos\delta_L \cos\delta \cos(\alpha_L - \alpha) \times \sin\delta_L \sin\delta - \sin^2 A_L \sin^2\delta_L \times \sin^2\delta = \cos^2\delta [1 - \cos^2(\alpha_L - \alpha)] \tag{37}$$

$$= \cos^2\delta - \cos^2\delta \cos^2(\alpha_L - \alpha) \tag{38}$$

$$\cos^2(\alpha_L - \alpha)(\cos^2\delta_s - \sin^2 A_L \cos^2\delta_L \cos^2\delta) - \cos(\alpha_L - \alpha)(2\cos\delta_L \cos\delta \sin^2 A_L \sin\delta_L \sin\delta) + (\sin^2 A_L - \sin^2 A_L \sin^2\delta_L \sin^2\delta - \cos^2\delta) = 0 \tag{39}$$

Let

$$\begin{aligned} A &= \cos^2\delta - \sin^2 A_L \cos^2\delta_L \cos^2\delta \\ B &= -2\cos\delta_L \cos\delta \sin^2 A_L \sin\delta_L \sin\delta \\ C &= \sin^2 A_L - \sin^2 A_L \sin^2\delta_s - \cos^2\delta_s \end{aligned} \tag{40}$$

Then

$$\cos(\alpha_L - \alpha_s) = \frac{-B \pm (B^2 - 4AC)^{1/2}}{2A} \tag{41}$$

Equation (41) enables the calculation of points for the curves of constant A_L The points are obtained in the same manner as the points for constant Φ, that is, choosing A_L and incrementing δ_s from $-90°$ to $+90°$

A remaining problem is that multiple answers are obtained in the A_L case as well as in the constant Φ case However, in the constant A_L case, four values of $(\alpha_L - \alpha)$ are obtained for each δ increment, and only two of these correspond to the desired A_L The other two correspond to the explement of the A_L used in Eq (41) To identify which $(\alpha_L - \alpha)$ go with the desired A_L and which to the explement of A_L, it is necessary to substitute each $(\alpha_L - \alpha)$ obtained from Eq (41) into Eq (14), obtaining

$$\cos\Phi = \cos\delta_L \cos\delta_s \cos(\alpha_L - \alpha) + \sin\delta_L \sin\delta \tag{42}$$

Then using Eq (17) and the Φ obtained in Eq (42), compute

$$\sin A_L = - \frac{\cos\delta \sin(\alpha_L - \alpha)_i}{\sin\Phi} \tag{43}$$

and obtain the $\cos A_L$ from Eq (23), still using $(\alpha_L - \alpha)$ and the Φ from Eq (42):

$$\cos A_L = (Q/|Q|)(1 - \sin^2 A_L)^{1/2} \tag{44}$$

From Eqs (43) and (44), A_L and its correct quadrant can be determined Each $(\alpha_L - \alpha_s)$ can be matched with A_L or the explement of A_L for identification of the curve

It is now possible to compute and identify in a straightforward manner all of the points necessary to draw the curves in Figs 2, 3, 7, and 8 Using these equations, it now appears that much of the remaining problem of earth-lunar trajectory design as outlined in the paper can be mechanized However, as it was the primary object of this comment to elaborate upon the subject paper by deriving the equations from which the lines of constant launch azimuth and constant central angle can be generated, the problem of mechanization of the trajectory design problem will not be pursued further

Reference

[1] Michaels, J E, "Design analysis of earth lunar trajectories: launch and transfer characteristics," AIAA J 1, 1342–1350 (1963)

Comments on Exhaust Flow Field and Surface Impingement

LEONARD ROBERTS* AND JERRY C SOUTH JR †
NASA Langley Research Center, Hampton, Va

Nomenclature

k = $\gamma(\gamma - 1)M_e^2$
h = distance along streamline from point source (nozzle exit)
r = radial coordinate normal to axis
r_e = nozzle exit radius
θ = streamline inclination angle relative to axis
M = Mach number
γ = ratio of ideal-gas specific heats
ρ = density
ρ_0 = nozzle stagnation density
ν = Prandtl Meyer turning angle
p_s = static pressure on surface beneath nozzle
p_{re} = normal shock recovery pressure at nozzle exit
p_0 = nozzle stagnation pressure

Subscripts

e = conditions at nozzle exit
a = conditions on axis

IN recent months there has been interest in the problem of the impingement of a jet exhaust on simulated lunar surfaces The problem has been described both experimentally[1] and theoretically [2 3] In the June issue of the AIAA Journal there appeared two Technical Notes[4 5] that seemed to complicate unnecessarily the analysis of the free-jet expansion and the surface pressure distribution The purpose of the present comment is to recall briefly the simple results of the theory[3] and to make a more complete comparison with the experimental data of Ref 1

First, with regard to the expansion of the free jet into a vacuum, most of the mass and momentum of the jet are contained in a central core in which the density decreases both along and normal to the axis, and at large distances the density distribution should be independent of the opening angle of the nozzle Furthermore, one would not expect

Received September 27, 1963
* Head, Mathematical Physics Branch Member AIAA
† Aerospace Engineer Member AIAA

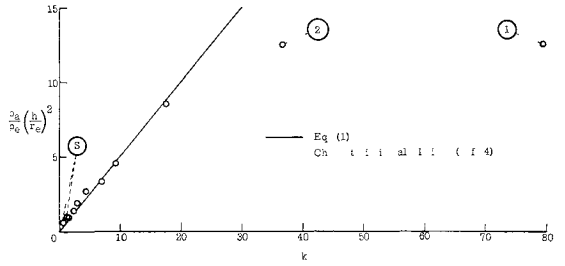

Fig 1 Far-field density distribution correlated with hypersonic parameter $k = \gamma(\gamma - 1)M^2$

the angle of the bounding streamline to be a significant parameter as suggested in Ref 4, since there the density is zero A simple analysis[3] shows that

$$\rho/\rho_e = (k/2)(h/r_e)^{-2}(\cos\theta)^k \tag{1}$$

where $k = \gamma(\gamma - 1)M_e^2$ is a single hypersonic parameter that will correlate jets of different Mach number and γ Physically, this parameter is interpreted as

$$\frac{k}{2} = \frac{\gamma(\gamma - 1)M_e^2}{2} = \frac{V_e^2/2}{c_v T_e}$$

$$= \frac{\text{exhaust gas kinetic energy}}{\text{exhaust gas internal energy}} \tag{2}$$

and its usefulness is demonstrated by the plot of Fig 1, where the value of $(\rho_a/\rho_e)(h/r_e)^2$ determined (on the axis, $\theta = 0$) by a characteristic net calculation[4] is shown as a function of k

Table 1 in Ref 4 lists 12 different nozzles together with calculations of the parameter $B = (\rho_a/\rho_0)(h/d^*)^2$ at locations far downstream from the nozzle exits For each case the nozzle area ratio A_e/A^*, exit angle θ_e, and γ were given Since the exit Mach number M_e was not given, the authors of the present note assumed the one-dimensional, area-Mach-number relation to hold in order to obtain M_e and finally k The parameter $(\rho_a/\rho)(h/r)^2$ was then computed using

$$\frac{\rho_a}{\rho}\left(\frac{h}{r}\right)^2 = \frac{4B}{(\rho/\rho_0)(A/A^*)}$$

$$= 4\left(\frac{2}{\gamma+1}\right)^{-(1/2)[(\gamma+1)/(\gamma-1)]} \times \left(\frac{\gamma-1}{2}\right)^{-1/2}\left(1 + \frac{2\gamma}{k}\right)^{-1/2} B \tag{3}$$

Two of the nozzles listed in Ref 4 were sonic nozzles (labeled

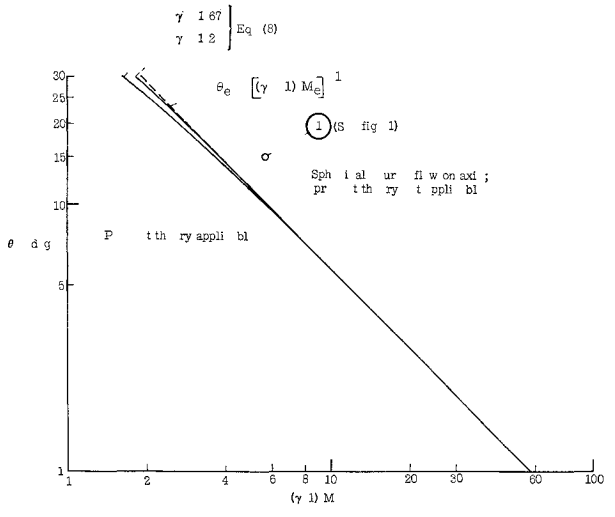

Fig 2 Region of applicability of present theory for conical nozzles

s in Fig 1) and are not expected to correlate well with the present theory The other nozzles, with the exception of the nozzle represented by point 1, are within the range of validity of the present theory Point 1 is not a typical far-field nozzle exhaust for the reasons stated below

The first right-running characteristic (leading characteristic) emanating from the lip of a supersonic nozzle carries with it the first disturbance signaling the corner expansion For a conical nozzle of semiangle θ, the first characteristic is curved and may never intersect the axis under certain conditions It may be assumed that isentropic, spherical, source-flow exists upstream of this line, and the shape of the characteristic can be obtained in closed form In particular, the flow angle along the characteristic is given by

$$\theta = \theta + \tfrac{1}{2}(\nu - \nu) \tag{4}$$

where ν is the Prandtl-Meyer turning angle,

$$\nu = \left(\frac{\gamma+1}{\gamma-1}\right)^{1/2}\tan^{-1}\left[\frac{\gamma-1}{\gamma+1}(M^2-1)\right]^{1/2} - \tan^{-1}(M^2-1)^{1/2} \tag{5}$$

If the characteristic intersects the axis downstream, then $\theta = 0$ at the intersection point, and the turning angle is

$$\nu_a = \nu_e + 2\theta \tag{6}$$

If ν_a exceeds the maximum turning angle ν_{max}, then the first characteristic does not intersect the axis but asymptotically coincides with one of the source-flow streamlines off the axis, at an angle

$$\theta = \theta - \tfrac{1}{2}(\nu_{max} - \nu) \tag{7}$$

All streamlines within this limiting cone are undisturbed by the corner expansion at the nozzle lip; thus spherical source flow will continue to exist on the axis to infinity Approximate solutions that account for both the axial and radial expansion in the far-field exhaust will not be valid on the axis for conical nozzles when

$$\nu_e + 2\theta \geqq \nu_{max} \tag{8}$$

or approximately for large M, when $(\gamma - 1)M > \theta^{-1}$

Figure 2 is a graphical representation of Eq (8), which implicitly defines the maximum exit Mach number for which the first characteristic of a given conical nozzle can intersect the axis The M_e of point 1 ($\gamma = 1.67$, $\theta = 15°$, $M = 8.43$) falls above this maximum, whereas all of the other conical-nozzle cases are well within range of the present theory The axis density distribution far downstream for nozzles which lie above the curve in Fig 2 is

$$\rho_a/\rho\,(h/r_e)^2 = [1 + (2\gamma/k)]^{-1/2}\csc^2\theta \tag{9}$$

or

$$B = \tfrac{1}{4}[2/(\gamma+1)]^{1/2[(\gamma+1)/(\gamma-1)]}[(\gamma-1)/2]^{1/2}\csc^2\theta \tag{10}$$

For the case of point 1, the limit value for B [Eq (10)] is 1.213, whereas a value of 1.04 was calculated in Ref 4 at $h/r = 50$ (an exact source-flow calculation gives $B = 1.06$ at $h/r = 50$), some 14% below the limit value Since the value of B given for point 2 ($\gamma = 1.67$, $\theta = 0$, $M = 5.72$) was also calculated at $h/r = 50$, it seems possible that the agreement with the present theory would be improved if the characteristics were carried farther downstream Aside from this, there is some doubt in the value of M (and thus k) computed for point 2, since one-dimensional flow is not strictly valid for bell ($\theta = 0$) nozzles

The pressure distribution that results on a surface placed beneath the jet and normal to its axis is also expressed very easily in terms of the hypersonic parameter k as follows[3]: For $(h/r)[2/(k+2)]^{1/2} > 1$,

$$p/p = [(k+2)/2](h/r)^{-2}(\cos\theta)^{k+4} \tag{11a}$$

For $(h/r_e)[2/(k+2)]^{1/2} \leqq 1$,

$$p_a/p = 1 \tag{11b}$$

where p_a, the normal shock recovery pressure, is approximately expressed in terms of the total stagnation pressure p_0 as

$$\frac{p_{re}}{p_0} = (1 + \gamma M^2)\left(1 + \frac{\gamma - 1}{2} M^2\right)^{-[\gamma/(\gamma-1)]}$$

Equation (11a) is found by taking the density distribution of Eq (2) and the flow velocity as its maximum value and computing the normal momentum flux against the surface At the stagnation point, $\cos\theta = 1$, and the pressure varies inversely as the square of the dimensionless height $(h/r)[2/(k+2)]^{1/2}$ For very small values of the height $\{(h/r)[2/(k+2)] \leqq 1\}$ this expression is clearly not applicable, and the pressure is better approximated by $p_a = p$ [Eq (11b)], the shock recovery pressure

Figure 3a shows the variation of p_a/p with $(h/r)[2/(k+2)]^{1/2}$ together with the data of Ref 1 for four nozzles of different exit Mach number and opening angle This plot again shows the significance of the parameter k and indicates that Eq (11a) can generally be applied when $h/r\,[2/(k+2)]^{1/2} \geqq 2$

The radial distribution of surface pressure is shown in dimensionless form in Fig 3b, where the data are plotted in the form p/p_a against $[(k+4)/2]^{1/2}(r/h)$ for various nozzles at various heights satisfying $\{(h/r)[2/(k+2)]^{1/2} \geqq 2\}$ The approximate theoretical expression is written

$$p/p_a = (\cos\theta)^{(k+4)/2} = [1 + (r/h)^2]^{(k+4)/2} \approx \exp -\{(r/h)[(k+4)/2]^{1/2}\}^2 \tag{12}$$

for large k, and this latter expression for p/p_a is shown as the solid curve There is some scatter in the data (part of which results from difficulty in reading the data accurately), but the agreement between experiment and theory is adequate for most engineering purposes

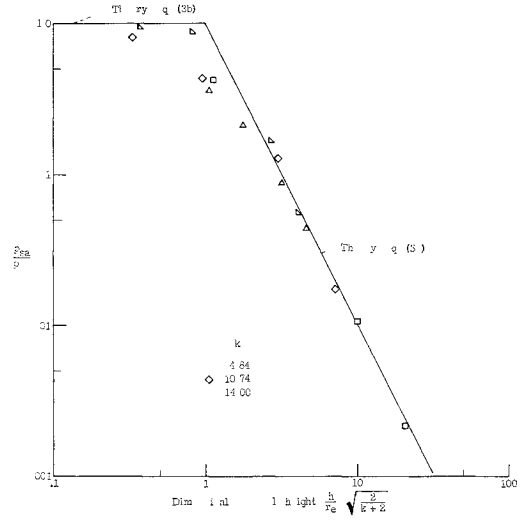

Fig 3a Variation of surface pressure with height

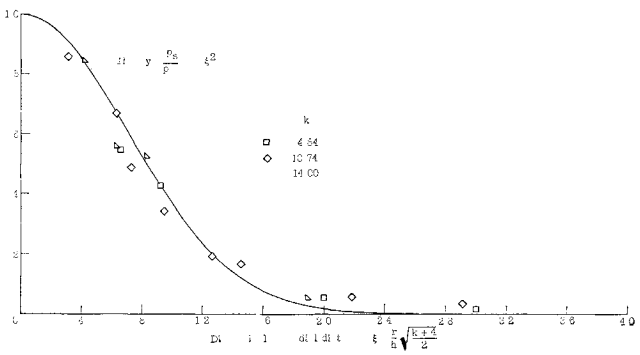

Fig 3b Surface pressure distribution

The restriction $(h/r)[2/(k+2)]^{1/2} \geqq 2$ is not considered a severe one since the vehicle is practically on the surface when $h = [(k+2)/2]^{1/2} r_e$ For typical values $k = 6$ and $r_e = 1$ ft, for example, the present theory [Eq (11a)] is valid until the vehicle descends to a height of 4 ft (i e , until the nozzle exit is 4 ft from the surface), and in practice it is expected that the vehicle will have cut off its thrust before reaching this height In view of the good agreement between the simple theory and the experimental data throughout virtually the complete range of heights of interest, there seems to be little advantage in using the more complicated method of Ref 5 to calculate surface pressure

The advantage of using the simpler form is that the surface pressure can be written in terms of the nozzle thrust Since $p = \text{thrust}/\pi r^2$, this expression, together with (11a) and (12), gives

$$p = \frac{\text{thrust}}{\gamma\{h[2/(k+2)]^{1/2}\}^2} \exp -\left\{[(k+4)]^{1/2}\left(\frac{r}{h}\right)\right\}^2 \tag{13}$$

which is independent of the nozzle dimensions and depends only on the nozzle thrust, the vehicle height, and the radial distance along the surface

References

[1] Stitt, L E , ' Interaction of highly underexpanded jets with simulated lunar surfaces," NASA TN D 1095 (1961)

[2] Roberts, L , Exhaust jet dust layer interaction during a lunar landing " Thirteenth International Astronautical Congress, Varna, Bulgaria (September 23–29, 1962)

[3] Roberts, L The action of a hypersonic jet on a dust layer," IAS Paper 63-50 (1963)

[4] Sibulkin M and Gallaher, W H , "Far field approximation for a nozzle exhausting into a vacuum, ' AIAA J 1, 1452–1453 (1963)

[5] Eastman, D W and Radtke, L P , Flow of an exhaust plume impinging in a simulated lunar surface,' AIAA J 1, 1430–1431 (1963)

Reply by Authors to L Roberts and J C South Jr

LEONARD P RADTKE* AND DONALD W EASTMAN*

The Boeing Company, Seattle, Wash

WHETHER our method for determining the flow field over a lunar surface subject to exhaust plume impingement is complicated or not is a relative question If one has a characteristics computer program for defining the exhaust plume properties, then the method is certainly quite straightforward If, however, one does not have a characteristics capability, then the method suggested by Roberts is useful

We would like to point out that the computer program used to obtain the results presented in our note was not written specifically for this application This program was one result of a study conducted to develop methods for calculating flow properties in exhaust plumes The application to impingement problems was intended to illustrate one of its many uses The advantage of the characteristics program lies in the fact that real gas equilibrium or nonequilibrium

Received February 21, 1964

* Research Engineer, Aerospace Division Member AIAA